Structure, Vol. 10, 1235–1248, September, 2002, ©2002 Elsevier Science Ltd. All rights reserved. PII S0969-2126(02)00838-9

Comparison of In Vivo Selection and Rational Design of Heterodimeric Coiled Coils

Katja M. Arndt,[1,2,4] Joelle N. Pelletier,[2,5] Kristian M. Müller,[1,4] Andreas Plückthun,[2,3] and Tom Alber[1,3]
[1]Department of Molecular and Cell Biology
University of California, Berkeley
Berkeley, California 94720
[2]Biochemisches Institut
Universität Zürich
Winterthurerstr. 190
CH-8057 Zürich
Switzerland

Summary

To investigate how electrostatic interactions restrict the associations of coiled coils, we improved a heterodimeric coiled coil (WinZip-A1B1) by in vivo selection and, alternatively, by rational design. Selection from libraries encoding variable edge (g and e) residues enriched g/e′ ion pairs, but the optimum selected heterodimers unexpectedly retained two predicted repulsive g/e′ pairs. The best genetically selected heterodimer displayed similar thermodynamic stability and specificity as a rationally designed dimer with predicted ion pairs at all edge positions. This rationally designed pair, however, was less effective than the best genetically selected pair in mediating dimerization in vivo. Thus, the effects of predicted charge pairs depend on sequence context, and complementary charges at the edge positions rationalize only a fraction of the sequences that form stable, specific coiled coils.

Introduction

Oligomerization is a critical feature in protein function and regulation. Consequently, many protein design approaches have engineered oligomerization domains in order to generate or enhance biological function. An important general challenge in protein design is to combine two different proteins or domains to create assemblies with new properties [1, 2]. The domains that mediate oligomerization must be stable, specific, and expressed efficiently. Thus, building heterologous oligomerization domains requires a deeper understanding of the interactions that restrict protein associations, as well as factors that determine expression and stability in vivo. This combination of high specificity and cellular compatibility is required for both natural and designed oligomerization modules.

One of the oligomerization domains used commonly in protein design is the α-helical coiled coil [3–6]. Coiled coils consist of two or more α helices that wrap around one another in a left-handed supercoil. Coiled-coil sequences are characterized by a repeat of seven amino acids, denoted a–g (Figure 1A). Most of the residues at positions a and d are hydrophobic, forming a characteristic 3,4 repeat, and residues at positions e and g are often charged [7, 8]. Charged residues at the g position often form interhelical ion pairs with residues at the e′ position of the next heptad of the neighboring helix. The simplicity and small size of this motif has made it a popular choice for designing protein fusions with defined oligomerization states [9].

Coiled coils are formed by 3%–5% of amino acids in proteins [10], and this abundance emphasizes the importance of specific pairing. In addition to the effects of matching core polarity [11], core packing [12], and irregularities in the heptad repeats [13], pairing specificity is thought to derive mainly from the balance of ionic interactions between neighboring helices. In both natural and designed two- and three-helical coiled coils, charge repulsions in the homooligomers that are relieved in the heterooligomers are sufficient to mediate specific associations [7, 14–16]. We call this idea the PV hypothesis, an abbreviation in reference to the name of the design by Kim and coworkers of an obligate heterodimeric coiled coil [14]. The abbreviation PV is defined in the title of [14]. This pair of peptides is identical except at the e and g positions, where one sequence contains Lys and the other sequence contains Glu. This peptide pair (like other similar pairs) forms a stable heterodimer in vitro.

When fused to heterologous proteins, however, designed dimeric and trimeric coiled-coil sequences based on the PV hypothesis did not efficiently mediate oligomerization due to degradation in *E. coli* (K.M.A., P. Pack, and A.P., unpublished results). These results emphasized gaps in knowledge about a number of factors—including the roles of the e and g residues, folding efficiency, aggregation, or proteolysis—that determine expression and stability of coiled coils in vivo. Previous genetic selection strategies have focused primarily on homodimeric coiled coils, with heterotypic contacts assayed by subsequent screening [17, 18]. To develop specific dimerization domains for use in vivo, we previously carried out a genetic selection based on functional association of two fragments of dihydrofolate reductase (DHFR) mediated by an attached heterodimeric coiled coil [19, 20]. We used this DHFR fragment complementation assay (Figure 1B) to screen two libraries of coiled coils against each other to identify the best heterodimer.

Library A contained the surface residues (b, c, and f positions) of the c-Jun leucine zipper, and library B contained the surface residues of the c-Fos leucine zip-

[3]Correspondence: plueckthun@biocfebs.unizh.ch (A.P.), tom@ucxray6.berkeley.edu (T.A.)
[4]Present address: Institut für Biologie, Universität Freiburg, Schänzle-str. 1, 79104 Freiburg, Germany.
[5]Present address: Département de Chimie, Université de Montréal, Montréal, Québec H3C 3J7, Canada.

Key words: coiled coil; leucine zipper; library selection; PCA; protein design; protein engineering; protein-protein interactions

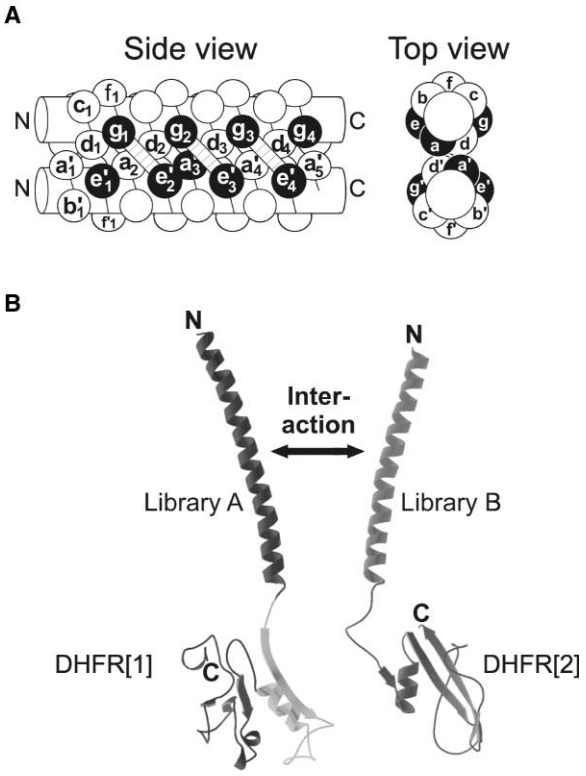

Figure 1. Overview of the Coiled-Coil Motif and the DHFR Protein Fragment Complementation Assay

(A) Schematic representation of a parallel, dimeric coiled coil in side and top views. The helical backbones are represented by cylinders, the side chains by knobs. The path of the polypeptide chain is indicated by a line wrapped around the cylinders. For simplicity, the supercoiling of the helices is not shown. Residues at positions a and d make hydrophobic contacts between the helices. Residues at positions e and g pack against the hydrophobic core and can participate in interhelical electrostatic interactions as indicated by the hatched bars. Positions varied in the libraries are shown in black. (B) The DHFR protein fragment complementation assay selects for heterodimer formation. Each library was genetically fused to one of the two DHFR fragments (DHFR[1] or DHFR[2]). Only an interaction between the two library peptides restores the DHFR enzymatic activity, which is crucial for cell survival under selective conditions. The Ile114Ala mutation in the DHFR fragment interface was used to increase selection stringency [52].

per. In both libraries, the core contained Leu at the d positions and Val at the a positions, except at the third a position (a3), which was a 1:1 mixture of Val and Asn for the system to select between specific association (Asn) and high interaction energy (Val). The e, g, and a3 positions were synthesized using trinucleotides [21] to encode equimolar mixtures of Arg, Lys, Gln, and Glu. The PV hypothesis predicted that the selected peptide pairs would be dominated by g/e′ ion pairs in the heterodimers and that the juxtaposed g and e′ residues would be devoid of repulsive ionic interactions. Unexpectedly, the selected winner sequences WinZip-A1 and WinZip-B1, which dominated the population after 12 serial passages, lacked fully complementary charged residues. The WinZip-A1B1 heterodimer even contained predicted repulsive residue pairs at two of the six juxtaposed g and e′ pairs (Figure 2). Nonetheless, WinZip-A1B1 formed a stable, specific heterodimer with a K_D of 24 nM at neutral pH. These results suggested that sequence solutions different from the PV hypothesis might be tolerated in heterodimeric coiled coils and that other factors may play a role in this selection result.

The apparent repulsive interactions in WinZip-A1B1 could derive from several factors, including incomplete sampling of the libraries, a failure of the selection to maximize heterospecificity, potential differences in protein expression levels, degradation, or failure of the PV hypothesis to comprehensively describe the role of electrostatic interactions. For example, the charged residues will interact with charges in the backbone, in the neighboring side chains, and with the helix dipole. In this report, we explore these possibilities by two distinct strategies: genetic selection and protein design. We selected novel partners from two "chain-shuffling" experiments and compared the outcome to a rational design based on the PV hypothesis. Both approaches started with the parental WinZip-A1B1 sequence. These experiments afforded the first direct comparison of rational design and selection methods for improving in vitro and in vivo performance of heterodimeric coiled coils. Interestingly, the selected pairs revealed a g/e′ interaction pattern, including charge repulsions, similar in character to the parental pair. A comparison of the thermodynamic stability of selected and designed pairs revealed only a minor influence of g/e′ pair repulsions compared to the dominant effects of the entire sequence context. These results indicate that the PV hypothesis, although correct, provides an incomplete picture of the contributions of the e and g residues to dimer stability and specificity. The discrepancy between in vitro and in vivo performance emphasizes the strength of in vivo approaches for selecting heterodimeric partners for use in in vivo applications.

Results

Improving WinZip-A1B1 by In Vivo Selection

The selection that yielded the original WinZip-A1B1 heterodimer covered a sequence space of only 2×10^6 out of 1.7×10^{10} possible combinations of the two helix libraries [19, 20]. Nevertheless, this selection included examples of all classes of charged and neutral amino acid pairs at the juxtaposed g and e′ positions. Statistical considerations argue that approximately 500 out of the 2×10^6 combinations sampled consisted of peptide pairs with complementary charges at all the juxtaposed g and e′ positions. Approximately 125 (25%) of these contained the preferred Asn pair at the core a3 position, suggesting that the two repulsive g/e′ interactions in WinZip-A1B1 were not simply the result of insufficient sampling [19]. To improve WinZip-A1B1 by in vivo selection, we performed two exhaustive chain-shuffling experiments. In each experiment, one helix of WinZip-A1B1 was kept constant and selected against the entire library (10^5) of complementary helices. Thus, helix A1 from WinZip-A1B1 was selected against the entire library B, and helix B1 was selected against the entire library A. The colonies resulting from the single-step

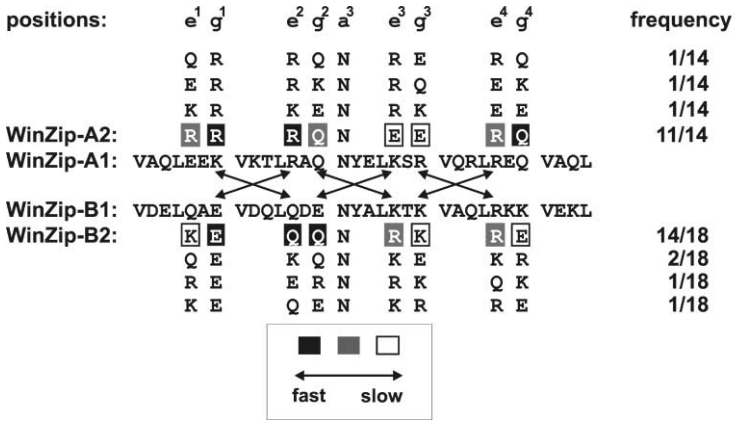

Figure 2. Sequences Obtained by Selection In Vivo

The sequences of the parental pair, WinZip-A1B1, are shown in the middle. The arrows indicate potential g/e′ interactions between the helices in the heterodimer. Above WinZip-A1 are the sequences selected in the chain shuffling of library A against WinZip-B1. The predominantly selected clone, WinZip-A2, was found 11 times out of 14 sequenced clones, as indicated by the frequency in the right hand column. Only the residues of the varied positions are shown. There were no changes in other positions. Below WinZip-B1 are sequences selected in the chain shuffling of library B against WinZip-A1. WinZip-B2 was found in 14 out of 18 sequenced clones. The boxes indicate the kinetics of the selection; the darker the box, the faster the selection rate (see Experimental Procedures).

selection on agar plates (see Experimental Procedures) were pooled into liquid medium, and growth competition was performed for 12 serial transfers (passages) under selective conditions. The sequences of pairs after passages 6, 8, 10, and 12 revealed that each chain-shuffling selection was dominated eventually by one pair (Figure 2). The newly selected pairs were named WinZip-A1B2 (selection of A1 against library B) or WinZip-A2B1 (selection of B1 against library A) [20]. In this nomenclature, the "2" in the name indicates the newly selected helix and "1" denotes the parental helix. The newly selected partners were closely related to WinZip-A1B1, with identical or similar (Lys/Arg exchange) residues in many of the varied positions.

Remarkably, the exhaustive selection procedure did not eliminate repulsive ion pairs at juxtaposed g and e′ positions. Each of the WinZip heterodimers retained two repulsive g/e′ pairs. Both in the parental sequence and WinZip-A1B2 these repulsive pairs occurred in the fourth heptad. In WinZip-A2B1, a repulsive pair in the fourth heptad was replaced by an attractive pair, and an attractive pair in the third heptad was replaced by a repulsive pair. Overall, the number of attractive g/e′ ion pairs was not increased by the chain-shuffling experiments. These results show that the occurrence of repulsive g/e′ pairs in the WinZip heterodimers did not result from insufficient sampling of the libraries.

Kinetics of In Vivo Selection

Insights into the selection process and the importance of the varied e and g positions were obtained by sequencing library pools after every second passage. The sequences of 26 clones from library A and 24 clones from library B before selection revealed the expected even distribution of amino acids (28% Gln, 22% Glu, 25% Lys, 25% Arg) at the varied e and g positions and the core a3 position (45% Val, 55% Asn). These values are close to the expected ratios for random incorporation of the trinucleotides. The trinucleotide codons (CAG coding for Gln; GAG coding for Glu; AAG coding for Lys; CGT coding for Arg) [21] at the varied positions in the DNA libraries allowed us to deconvolute the sequencing profiles of pools of clones to determine the ratio of the corresponding amino acids in each passage.

One amino acid dominated at all the varied positions in the later passages (Figure 2). The rates of convergence to this predominant sequence, however, varied significantly between different positions. Figure 3 shows the kinetics of selection for the chain shuffling of WinZip-B1 against library A. In the progenitors of WinZip-A2, for example, the CGT codon for Arg at position g1 was already well represented in the single-step selection (P0), and Arg dominated clearly after the first passage (Figure 3). In contrast, Glu at position g3, which forms putative ion pairs with Arg residues at e4 in both the homodimer and heterodimer, did not dominate the population until passage six.

In early passages of both chain-shuffling experiments, Gln was most abundant at most positions (e.g., Figure 3). Since the four amino acids (Gln, Glu, Lys, and Arg) were equally represented at the e and g positions before selection, an enrichment for Gln residues must have occurred in the single-step selection. This pattern may be explained by the "neutral" character of Gln, which precludes charge repulsions. This permissive character, coupled with relatively high helical propensity [22], can mediate many stable pairings that fulfill the demands of the single-step selection. A disadvantage of Gln, however, is the lack of heterospecificity due to the absence of repulsive g/e′ pairs in the homodimers. This effect may account for the loss of Gln-rich pairs and the enrichment of charged e and g residues in the later passages. This idea is consistent with our previous observation that selection for stability is observed even in the lowest stringency selection, whereas selection for heterospecificity is more pronounced in the higher stringency selections [19].

The only exception to the predominance of Gln in the early passages was at position e2 in the chain-shuffling experiment that produced the winner WinZip-A2B1 (Figure 3). In this case, positively charged amino acids (Arg and Lys) already dominated in P0. This position is conserved between the chain-shuffling winner and the parental sequence, and it is selected at a fast rate.

Among the three charged amino acids used in the randomization scheme, Glu was underrepresented after the single-step selection (P0) of both chain-shuffling experiments. Overall, Glu was selected against more

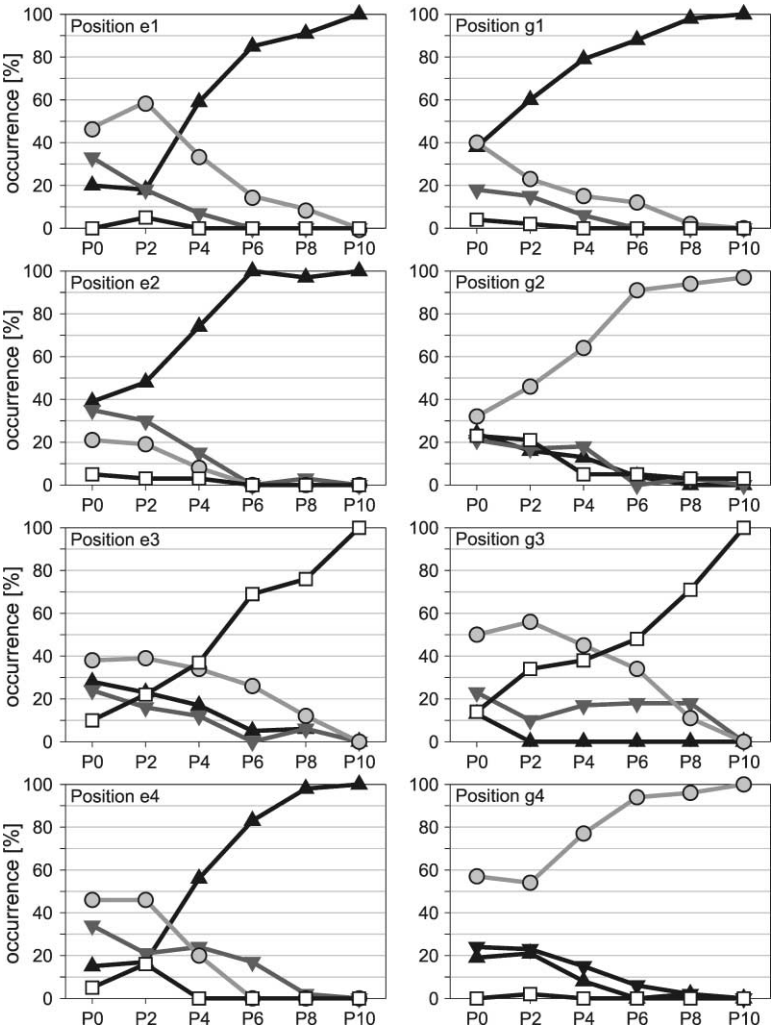

Figure 3. Different Rates of Selection at Each Position in WinZip-A2

The percent of each amino acid found at each varied position is plotted as a function of passage number. Pools were sequenced after every other round of competition selection (▲, black = Arg [CGT]; ▼, dark gray = Lys [AAG]; ○, light gray = Gln [CAG]; □, white = Glu [GAG]). P0 indicates the sequence of the library A pool after the single-step selection before the first passage of growth competition. Residues conserved in WinZip-A1 and WinZip-A2 tended to dominate the pool earlier in the selection.

rapidly than the residues Lys and Arg. Two exceptions to this trend were observed: (1) positions where Glu was specifically selected (e3 and g3 in WinZip-A2 [Figure 3] and g1 and g4 in WinZip-B2); (2) positions where Glu was not ultimately selected but which pair with positively charged residues in the other helix (g2 and e4 in library A, which pair with Lys in WinZip-B1 [Figure 3] and g2 and g3 in library B, which pair with Lys and Arg, respectively, in WinZip-A1). These trends suggest that, except for cases where Glu can make beneficial interactions, Glu appears to have a more deleterious effect than Lys or Arg.

Biophysical Analysis of the Selected Pairs

To investigate the energetics of pairing of the selected sequences, the peptides corresponding to the parental pair, WinZip-A1 and WinZip-B1, and the two selected chain-shuffling winners, WinZip-A2 and WinZip-B2, were synthesized and analyzed in vitro. The peptides were characterized alone and in equimolar mixtures that formed the heterodimers WinZip-A1B1, -A1B2, and -A2B1. A detailed analysis of the parental pair WinZip-A1B1 has been described previously [19].

The peptides were α helical alone and in combination, as demonstrated by the characteristic minima in the circular dichroism (CD) spectra. The estimated α-helical contents at 5°C varied from 85% to 100% (Table 1). The helix content of the WinZip-B2 homodimer (92%) was higher than that of the parental homodimer (85%). To assess stability and heterospecificity, thermal and urea denaturation experiments were performed (Figure 4; Table 1). The WinZip-A2 and WinZip-B2 homodimers were slightly more stable than the parental homodimers. When comparing the heterodimers, no significant difference in stability was seen between WinZip-A1B1 and WinZip-A1B2, although the optimized sequence was more helical. In contrast, the second chain-shuffling winner, WinZip-A2B1, was significantly improved in vitro relative to the parental pair. WinZip-A2B1 showed increased stability (T_m = 63°C, K_D = 4.5 nM, ΔG = 11.2 kcal/mol) and heterospecificity (ΔT_m = 22.3°C, $\Delta\Delta G_{spec}$ = 3.2 kcal/mol) compared to WinZip-A1B1 (T_m = 55°C, K_D = 24 nM, ΔG = 10.2 kcal/mol, ΔT_m = 16.7°C, $\Delta\Delta G_{spec}$ = 2.6 kcal/mol).

Heterospecificity also was visualized by native gel electrophoresis (Figure 5). All three peptide combinations (WinZip-A1B1, -A1B2, and -A2B1) formed mainly heterodimers, as demonstrated by the predominant sin-

Table 1. Stability and Growth Properties of Selected and Designed Coiled Coils

	In vitro properties										In vivo properties	
							Type of e/g interactions					
Peptide pair	T_m (°C)	ΔT_m (°C)[a]	α helix content (%)[b]	K_D	ΔG (kcal/mol)	$\Delta\Delta G_{spec}$ (kcal/mol)[c]	+/+ or −/−	+/−	n/+	n/−	Relative colony size on agar plates (37°C; Figure 7)	Doubling time in liquid medium (hr)
VelB1	(26.4)[d]		67%	(6 μM)	7.0		4	2	—	—		
WinZip-B1	(27.6)[e]		85%	(73 μM)[e]	5.5		2	2	—	2		
WinZip-B2	28.1		92%	(5 μM)	7.1		2	—	2	2		
VelA1	45.6		82%	(63 nM)	9.7		4	2	—	—		
WinZip-A1	49.5[e]		100%	63 nM[e]	9.7		4	—	2	—		
WinZip-A2	54.2		101%	17 nM	10.4		2	2	—	2		
WinZip-A1B2	52.6	13.8	109%	40 nM	9.9	1.5	2	1	3	—	57%	
WinZip-A1B1	55.2[e]	16.7[e]	98%	24 nM[e]	10.2	2.6	2	2	2	—	100%	1.86 ± 0.07
WinZipA1-VelB1	55.7	17.8	99%	ND	ND	ND	2	3	1	—	181%	
WinZip-A2B1	63.2	22.3	99%	4.5 nM	11.2	3.2	2	2	2	—	320%	1.39 ± 0.02
VelA1-VelB1	69.2	33.2	87%	2.3 nM	11.6	3.3	—	6	—	—	250%	1.60 ± 0.02
VelA1-WinZipB1	70.0	33.4	88%	ND	ND	ND	—	5	1	—	190%	

Except for the WinZip-A2 homodimer, the sequence combinations are listed in order of increasing thermodynamic stability.

[a] $\Delta T_m = T_m$ (heterodimer) − [T_m (homodimer A) + T_m (homodimer B)]/2.

[b] Helix content was calculated according to [23].

[c] $\Delta\Delta G_{spec} = \Delta G$ (heterodimer) − [ΔG (homodimer A) + ΔG (homodimer B)]/2.

[d] Values in parentheses are only estimates because of low stability.

[e] Data were published previously [19].

ND, not determined.

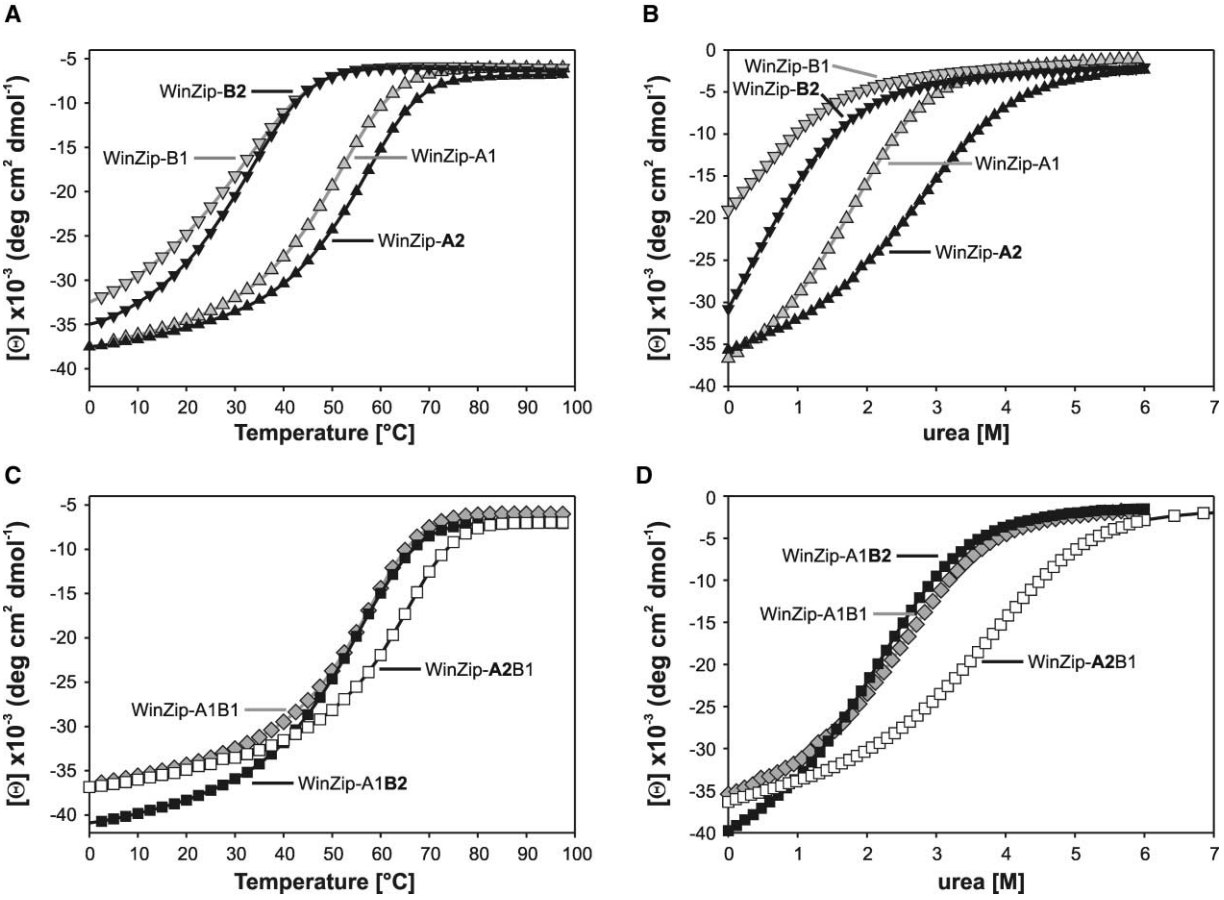

Figure 4. The In Vivo-Selected Pairs Form Stable, Specific Dimers

Thermal (A) and urea (B) denaturation of the homodimers WinZip-A1 (△, gray), WinZip-A2 (▲, black), WinZip-B1 (▽, gray), and WinZip-B2 (▼, black). Thermal (C) and urea (D) denaturation of the heterodimers WinZip-A1B1 (◇, gray), WinZip-A1B2 (■, black), and WinZip-A2B1 (□, white). Data from WinZip-A1B1 and the respective homodimers have been published previously [19]. Despite the presence of two, predicted, repulsive g/e′ pairs, WinZip-A2B1 formed the most stable and specific heterodimer obtained by in vivo selection.

gle band of intermediate mobility compared to the respective homodimers. The presence of a single hybrid band also demonstrated the absence of higher order species. Under the conditions used for electrophoresis, WinZip-A1B1 and WinZip-A1B2 showed a light smear, indicating dissociation of the heterodimers during the experiment. No smear was visible for WinZip-A2B1, consistent with its high stability and specificity (Table 1).

Improvement of WinZip-A1B1 by Rational Design

The complex patterns of charged residues obtained from the in vivo selection raised the question of how the selected sequences would compare with variants lacking repulsive g/e′ pairs. To explore this question, we altered WinZip-A1B1 by rational design (Figure 6A). Design considerations were based on the principle of maximizing g/e′ charge repulsion in the homodimers with concurrent relief upon heterodimer formation (the PV hypothesis). This pattern was achieved by changing the two charge repulsions in WinZip-A1B1 (Arg-Arg at g3[WinZip-A1]-e′4[WinZip-B1]) and Arg-Lys at e4[WinZip-A1]-g′3[WinZip-B1]) to Glu-Arg and Glu-Lys, respectively. Both mutations were placed in WinZip-A1 rather than in WinZip-B1 because of the higher stability of the WinZip-A1 homodimer (Figure 4; Table 1). To maximize heterodimer stability and specificity, the two neutral-charged interactions Lys-Gln (g1[WinZip-A1]-e′2 [WinZip-B1]) and Gln-Lys (g2[WinZip-A1]-e′3[WinZip-B1]) in WinZip-A1B1 also were replaced by Lys-Glu and Glu-Lys interactions, respectively. The Gln to Glu mutation at position e2 in WinZip-B1 also introduced two more repulsive pairs in the WinZip-B1 homodimer, which should increase specificity. The two designed helices based on WinZip-A1 and WinZip-B1 are named VelA1 and VelB1 (Figure 6A), respectively.

Biophysical Analysis of Rationally Designed Pairs

Peptides corresponding to VelA1 and VelB1 were synthesized and the stabilities of the homo- and heterodimer combinations were measured (Figures 6B and 6C). The CD denaturation curves of the heterodimers (Figure 6C) showed that the design improved stability (T_m = 69°C for VelA1-VelB1; T_m increased by 14°C and ΔG changed by 1.4 kcal/mol relative to WinZip-A1B1).

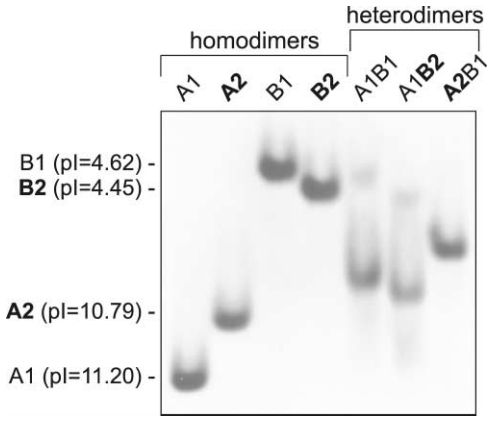

Figure 5. Preferential Heterodimer Formation by the WinZip Peptides

Native gel electrophoresis of the peptides WinZip-A1, -A2, -B1, and -B2 and the heterodimers WinZip-A1B1, -A1B2, and -A2B1 shows that the individual dimers were well resolved due to their different isoelectric points. Under the conditions used (pH 4.5, 5°C), WinZip-A1B1 and WinZip-A1B2 show a light smear, indicating breakdown of the heterodimers during electrophoresis. This smear is not visible in WinZip-A2B1, consistent with the high stability of the heterodimer.

The rationally designed pair showed slightly higher stability and specificity in vitro than the best in vivo-selected heterodimer, WinZip-A2B1 (Figure 4; Table 1).

The single mutation in VelB1 (Gln to Glu at position e2) was designed to destabilize the homodimer by adding a g/e′ repulsion. This substitution significantly lowered the helix content of the homodimer of VelB1 (67%) compared to the parental homodimer, WinZip-B1 (85%; Figure 6B; Table 1). This effect may be explained by fraying of the N terminus of the homodimer. Although this low stability made the equilibrium constants difficult to derive accurately, the overall stabilities of the WinZip-B1 and VelB1 homodimers appear to be in the same range. In heterodimers, the VelB1 and WinZip-B1 peptides showed comparable stabilities and helix contents. This effect was seen by comparisons of WinZip-A1B1 with WinZipA1-VelB1 or of VelA1-WinZipB1 with VelA1-VelB1 (Figure 6C; Table 1). Thus, the single substitution introduced to create VelB1 showed only limited effects in vitro.

Both WinZip-A1 and the triply substituted VelA1 contained four predicted g/e′ pair repulsions in the homodimers (Figure 6). The VelA1 homodimer, however, was less stable and less helical than the parental WinZip-A1 homodimer. Strikingly, the helix content of all combinations containing VelA1 was significantly reduced compared to the dimers containing the WinZip-A1. Nonetheless, the heterodimers containing VelA1 showed the highest apparent stabilities (Table 1; Figure 6C).

In Vivo Performance of Selected and Designed Heterodimers

Because one of our goals was to create specific heterodimers that function efficiently in a cellular environment, it was important to compare the performance of all the improved pairs in vivo. For this purpose, genes for the rationally designed sequences were cloned using the same codons as for the selected pairs and expressed in the fusions to mDHFR fragments used previously for the selection experiments. Growth rates were compared directly by plating aliquots of log phase cultures under selective conditions and determining the sizes of the resulting colonies. Colony size correlates with cell growth, which in turn is related to the efficiency of helix-mediated DHFR fragment complementation [20]. Plates were incubated at three different temperatures, 30°C, 37°C, and 42°C, and images of representative Petri dishes were scanned to quantify colony sizes (Figure 7).

The various constructs showed significant differences in average colony size (Figure 7). After incubation at 37°C, the best pair selected in vivo, WinZip-A2B1, produced the largest colonies compared to the other heterodimers (Figure 7; Table 1). The same rank order was observed at 42°C and 30°C, although the variation was less pronounced at the lower temperature (Figure 7C; Table 1). In accordance with the thermodynamic data, WinZip-A2B1 was superior to the parental pair and the other chain-shuffling pair, WinZip-A1B2. WinZip-A2B1 also grew faster than the rationally improved pair, VelA1-VelB1, which showed slightly greater stability and specificity in vitro.

To eliminate the possibility that the apparent superiority of WinZip-A2B1 was specific to the colony size assay, we measured growth curves in minimal medium under selective conditions at 37°C (Table 1). Two independent experiments were performed in triplicate or quadruplicate. Consistent with the plate assays, doubling times in solution were 1.86 ± 0.07 hr for WinZip-A1B1, 1.39 ± 0.02 hr for WinZip-A2B1, and 1.60 ± 0.02 hr for VelA1-VelB1. These assays confirmed that WinZip-A2B1 mediates faster growth than VelA1-VelB1.

Discussion

Complementary electrostatic interactions in many protein-protein interfaces are thought to confer specificity. Interfacial electrostatic interactions are complex, however, in part due to the many charged residues that participate over relatively long distances and the differences in shielding in the competing interfaces and solvent [24–27]. A simpler view, which we call the PV hypothesis, has been proposed to account for the restricted pairing of many α-helical coiled coils. In coiled coils, complementary charge pairs on the edge of the interface that relieve repulsive pairs in alternate oligomers are sufficient to promote formation of heterooligomers in natural and designed sequences [14, 16, 28–31]. Although not meant to embody physical or structural details, this idea successfully predicts the pairing preferences of some [31–33] but not other [17, 18, 34] coiled coils.

Here we tested the PV hypothesis by directly comparing rational design and genetic selection strategies to improve a previously selected, heterodimeric coiled coil, WinZip-A1B1. Both strategies led to significantly improved pairs with higher stability and specificity in vitro. Contrary to the PV hypothesis, the WinZip heterodimers selected in vivo neither maximized predicted, attractive, g/e′ charge pairs nor eliminated predicted, repulsive, g/e′ charge pairs. The best sequence pair obtained by

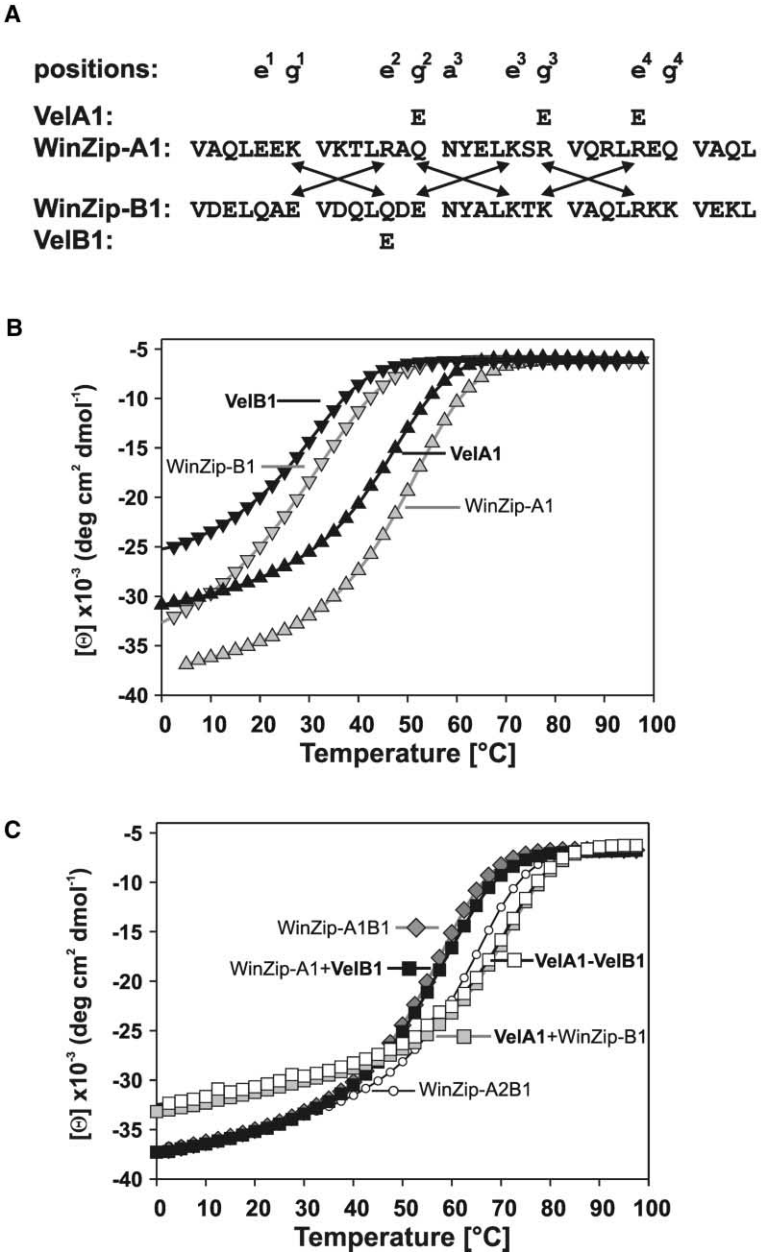

Figure 6. The Rationally Designed Pair VelA1-VelB1 Formed the Most Stable, Specific Heterodimer In Vitro

(A) The sequences of the parental pair, WinZip-A1B1, are shown in the middle. The changes in the rational design of VelA1 and VelB1 with respect to the parental pair are indicated above and below the WinZip-A1 and -B1 sequences, respectively. Arrows indicate g/e′ ion pairs predicted in the heterodimer. The designed heterodimer contains six predicted g/e′ ion pairs and each homodimer contains four predicted repulsive g/e′ pairs.

(B and C) Thermal denaturation followed by CD at 222 nm of the rationally designed dimers and the parental sequences, WinZip-A1 and WinZip-B1.

(B) Homodimers WinZip-A1 (△, gray), VelA1 (▲, black), WinZip-B1 (▽, gray), and VelB1 (▼, black).

(C) Heterodimers WinZip-A1B1 (◇, gray), WinZipA1-VelB1 (■, black), VelA1-WinZip-B1 (□, gray), and VelA1-VelB1 (□, white).

in vivo selection, WinZip-A2B1, was nearly as stable in vitro as the rationally improved pair, VelA1-VelB1 (Table 1). These results were unexpected, because WinZip-A2B1 retained two predicted, repulsive, g/e′ charge pairs, while VelA1-VelB1 contained six attractive pairs and no repulsive pairs. In combination with the reduced stability of the VelA1 homodimer, the VelA1-VelB1 heterodimer showed a modest gain in specificity in vitro. Despite the enhanced specificity and marginally higher stability of VelA1-VelB1 in vitro, this rationally improved pair was not the best heterodimerization domain in vivo.

Deviations from the PV Hypothesis

Biophysical studies of the various peptide pairs enabled us to investigate the influence of the g/e′ residues in detail. The number of predicted g/e′ charge repulsions, for example, did not correlate directly with the in vitro stability of the homo- and heterodimers. This trend was apparent, for example, from the fact that different peptide pairs with a total of two charge repulsions displayed T_m values under identical conditions ranging from 28°C to 63°C. Similarly, the difference in T_m between WinZip-A1B1 and WinZip-A2B1, which both have two repulsive g/e′ pairs, is larger than the difference in T_m between WinZip-A2B1 and VelA1-VelB1, which have two and zero repulsive g/e′ pairs, respectively. Despite the considerable variations in stability, the number of potentially repulsive, neutral, and attractive g/e′ interactions remained similar for all the WinZip-AB heterodimer pairs (Table 1). Strikingly, the significant improvement obtained in WinZip-A2B1 did not require elimination of potentially repulsive interactions. These results suggest

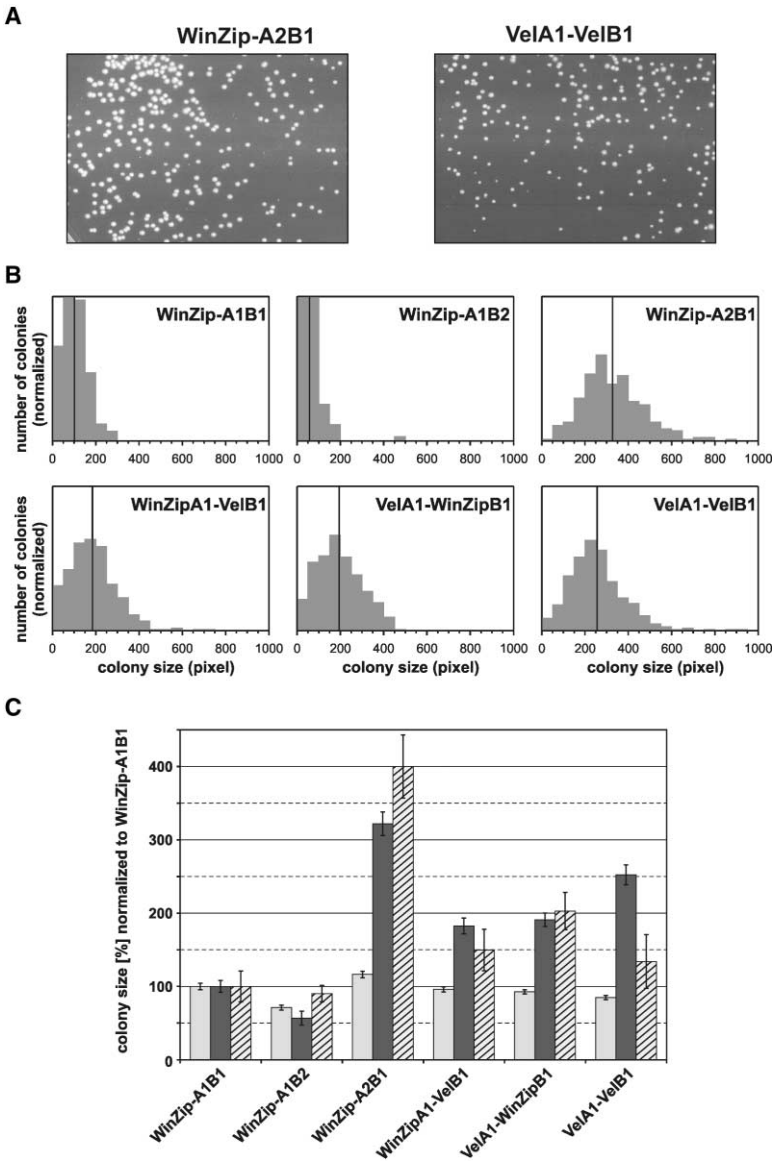

Figure 7. DHFR Fusions of the WinZip-A2B1 Combination Obtained by Chain Shuffling In Vivo Conferred the Fastest Cell Growth

Six heterodimeric DHFR fusions were compared at 30°C, 37°C, and 42°C.

(A) Colonies from the best chain-shuffling combination, WinZip-A2B1, and the designed pair, VelA1-VelB1, on selective agar plates incubated at 30°C.

(B) Quantification of the colony sizes from selective agar plates incubated at 37°C. The colony areas were grouped into bins of 50 pixels, and the number of colonies in each bin was plotted against the colony size. The vertical black line indicates the mean.

(C) Mean colony sizes obtained after incubating selective agar plates at 30°C (light gray), 37°C (dark gray), and 42°C (hatched) normalized to WinZip-A1B1. Due to the small colony sizes at 42°C, background dots led to an overestimate of the number of small colonies. The error bars indicate the 95% confidence interval.

that there is more variation in the contributions of g/e′ ionic residues than is accounted for simply by counting the number of predicted attractive and repulsive pairs.

A variety of factors could influence the contributions of g/e′ ionic residues. The overall electrostatic potential, including inter- and intramolecular interactions, plays a major role [24–27]. Interactions with the core residues, such as favorable packing or steric clashes, also have been proposed to modulate g/e′ interactions [35, 36]. Other effects of the sequence context may arise from local helix flexibility or from interactions with b, c, or f residues [19, 37]. Examination of coiled-coil structures also suggests that the e and g positions are structurally different, and these differences may accommodate specific charge pairs in different ways [38–40].

With the exception of WinZip-A2 and WinZip-A1B2, the homo- and heterodimers were sorted in Table 1 by increasing thermal stability. This procedure automatically grouped the peptides according to their origin. Library B-derived homodimers formed the least stable group, followed by library A homodimers. With one exception, the heterodimers formed the most stable group (Table 1). The differences between these groups, apart from the g/e′ pairs, reside in the solvent-exposed positions b, c, and f. Thus, these surface positions are crucial for the overall dimer stability.

The global differences in dimer stability could not be rationalized in terms of the amino acid content of the peptides alone. We assessed the tendency of each peptide to form a monomeric helix, for example, using the program AGADIR [41, 42]. The underlying assumption was that regions with high helix forming tendency would favor formation of the helical dimer. AGADIR predicted only a low helix content of 0.5%–7.2% (at 37°C and 0.15 M ionic strength) in the selected and rationally improved coiled coils. The predicted helix contents did not correlate with relative stabilities. Similarly, summing the helical propensities derived by O'Neil and DeGrado from

the effects of substitutions at an f position of a coiled coil [22] predicted comparable stabilities for all the dimers. Thus, sequence-dependent factors, including inter- and intrahelical interactions, are likely to determine dimer stability.

Relatively little is known about the influence of the b, c, and f positions on coiled-coil stability. Yu and coworkers suggested that intrachain repulsions between (i, i + 5) e and b residues decrease stability, although the destabilizing effect was less than for interchain g/e′ pair repulsions [43]. Increasing helix propensity at several surface positions stabilized the GCN4 coiled coil [44–46]. Based on the effects of mutations at b, c, and f positions of the GCN4 coiled coil, Dahiyat and coworkers concluded that helix propensity was more important for stability than hydrogen bond formation and polar hydrogen burial [47]. In contrast to this trend, the c position substitution, Arg25Ala, which perturbed a c-g-e′ salt bridge network in the GCN4 leucine zipper, decreased dimer stability [37]. Similarly, introducing intrahelical salt bridges involving 3 residues (f_i-c_{i+4}-f_{i+7}) stabilized the GCN4 leucine zipper [44]. A new c-g-e′ triplet of complementary charges was introduced into WinZip-A2B1 by the Arg-to-Glu change in position g3. WinZip-B2 contains the potential for a new c-g intrahelical salt bridge in heptads 4–5. These diverse results emphasize the importance of the overall electrostatic potential of the system, rather than specific ion pairs.

In the alternative, rational design strategy, the PV hypothesis guided the choice of mutations in WinZip-A1 and WinZip-B1 that simultaneously introduced a total of six, predicted, g/e′ ion pairs in the heterodimer and four repulsive g/e′ charge pairs in each homodimer. These mutations were unlikely to be purely advantageous. The introduction of the two negative charges close to the C terminus was likely to destabilize the homo- and heterodimers because of an unfavorable interaction with the helix dipole [48]. Furthermore, increasing the number of Glu residues, which show relatively lower helix propensity, was expected to decrease both homo- and heterodimer stability [22, 49]. Considering previous successful, rational designs of heterodimers [14, 40, 50], however, the gain in stability from replacing the two g/e′ charge repulsions in the parental heterodimer with two ion pairs might outweigh any destabilizing effects. In fact, Vel-A1B1 was stabilized by ~10-fold relative to the parental heterodimer (Table 1). In addition, the VelA1 homodimer was weakly destabilized relative to the parental homodimer (Table 1). The combination of these effects yielded an increase in the specificity of heterodimer formation. Thus, the specificity of the sequence combinations coincides qualitatively with the PV hypothesis, but it also shows that a more sophisticated treatment is needed to fully understand the effects of sequence changes.

It would be incorrect to conclude, however, that the presence of predicted repulsive g/e′ charge pairs precludes stable dimer formation. The VelA1-VelB1 and WinZip-A2B1 heterodimers, for example, displayed similar dissociation constants despite the presence of two putative repulsive pairs in the WinZip-A2B1 heterodimer (Table 1). These results suggested that similarly charged residues in juxtaposed g and e′ positions can be tolerated in certain contexts. In addition, simple tabulation of predicted attractive and repulsive g/e′ charge pairs in alternate dimers did not provide a general predictor of pairing preferences of the WinZip sequences. In this sense, the PV hypothesis does not account for numerous sequence combinations that may form stable coiled coils.

In Vitro Stability and In Vivo Selection

Despite the improved stability and specificity of VelA1-VelB1 in vitro, the rationally designed heterodimer, when fused to mDHFR fragments, conferred slower growth than the optimized WinZip-A2B1 heterodimer selected in vivo (Table 1; Figure 7). These results suggest that in vivo function depends on factors in addition to stability and specificity. The rationally improved sequences, for example, showed reduced helix contents. This reduction in helix content may compromise function by decreasing the alignment of the DHFR fragments or increasing proteolysis of the fusion proteins. Other effects, such as adventitious interactions with host coiled coils, may also contribute to the reduced in vivo function of the rationally modified pair.

The chain-shuffling experiments provided valuable information about how both helices in WinZip-A1B1 could be improved. Compared to WinZip-B2, WinZip-A2 contained more differences from the parental sequence and conferred a greater increase in stability in vitro. Considering only the six positions that participate in interhelical g/e′ pairs (Figure 1), WinZip-B2 has only one sequence change compared to B1 (Glu to Gln at position g2). Curiously, WinZip-B2 reduced the specificity and stability of the heterodimer with WinZip-A1. In addition, the WinZip-A1B2 heterodimer in the DHFR fusion conferred slower growth than the parental sequence in vivo. These results raise the question of how the WinZip-B2 sequence emerged from the chain-shuffling experiment. It is possible that the chain-shuffling protocol was relatively insensitive to the small differences in the properties of the WinZip-B1 and WinZip-B2 sequences. In this model, the lack of significant improvement by chain shuffling suggests that the WinZip-B1 helix selected originally was already a nearly optimal partner to WinZip-A1. Alternatively, the increased helix content of WinZip-B2 (Table 1) may have conferred an advantage in the chain-shuffling selection.

In contrast, WinZip-A2 has three changes in the six juxtaposed e and g residues compared to WinZip-A1. The three substitutions include one apparently conservative change (Lys to Arg at position g1) and two charge reversals (Lys to Glu at position e3, and Arg to Glu at position g3). These changes were associated with increased in vitro stabilities of both the WinZip-A2 homodimer and the WinZip-A2B1 heterodimer relative to the parental dimers. The specificity of the WinZip-A2B1 heterodimer (3.2 kcal/mol) was increased relative to the parental sequences (2.6 kcal/mol). This improvement in specificity is over and above the increased stability of the WinZip-A2 homodimer (Table 1), reflecting a specific, nonadditive advantage of the interhelical pair. These results emphasize the ability of genetic selection to provide unanticipated solutions to biochemical problems.

Kinetics of Selection

The kinetics of the selection in the chain-shuffling experiments provided information about the importance of the various randomized positions. The use of trinucleotide codons for residue randomization afforded a strategy for determining residue ratios in the population that was considerably faster than sequencing many individual clones. A strong correlation was observed between the selection rate and the variability of the residues. Residues that are identical or similar between the parental and the newly selected helices were in most cases selected at fast rates. This effect was most apparent at the core a3 position, which was randomized to Val and Asn. We observed previously that an Asn pair at this position is strongly selected (>90%), even in the single-step selection [19]. The same holds true in both chain-shuffling experiments. Among the g/e′ pairs, the two g/e′ pairs closest to the N termini are identical or similar in the parental pair and the two newly selected pairs. Residues at these positions were selected at a fast rate, suggesting the importance of these two interactions relative to other g/e′ pairs. The correlation between rapid selection and the positions of similarity in the parental and improved sequences suggests that the selection kinetics report on the importance of each position for heterodimer formation. These results emphasize the conclusion that the g/e′ pairs along the helix apparently make unequal contributions to stability or specificity.

In the WinZip heterodimers, the rapidly selected, conserved positions formed either opposite charged or neutral pairs in the N-terminal half of the coiled coil. The more slowly selected positions in the C-terminal half contained the same charged pairs. One explanation could be that the C-terminal part is actually destabilized in the in vivo selection in order to extend the linker to the DHFR fragments. This explanation is unlikely, since the selection experiments generally increased dimer stability and helix content. In addition, the 15- or 14-amino acid linker between the helix and the DHFR fragment is sufficiently long to allow the DHFR fragments to complement each other without steric hindrance [19]. Thus, the evidence supports the idea that the N-terminal region may comprise the most stable segment of the selected heterodimers, which is thus of most crucial importance in the selection experiment. This conclusion is consistent with studies of the GCN4 leucine zipper showing that the region that is most stable to hydrogen exchange also is most susceptible to helix-destabilizing mutations [37, 45, 46].

Applications of Improved Coiled-Coil Heterodimers

The properties of WinZip-A2B1 suggest that this dimer has great potential as a general, independent heterodimerization module for many in vivo applications. The DHFR fusion to WinZip-A2B1 afforded the fastest colony growth compared to the other pairs. The superiority of WinZip-A2B1 in vivo from 30°C to 42°C indicated that the selection optimized the coiled coil for a range of growth conditions. Different hosts or different protein fusions, however, may impose distinct sequence requirements. We recently evaluated the general usefulness of WinZip-A2B1 for heterodimerization [51]. An antibody Fv fragment was stabilized by substituting the constant domains of a Fab fragment with WinZip-A2B1, creating a helix-stabilized Fv (hsFv) antibody fragment. The expression, purification, oligomerization behavior, and stability of this Fv-WinZip-A2B1 fusion compared favorably with the properties of alternate Fv constructs. These results support the general utility of WinZip-A2B1 for dimerization in *E. coli*.

Conclusions

These experiments allowed for the first time a direct comparison between in vitro design and in vivo selection of heterodimeric coiled coils. The results demonstrate the power and importance of the in vivo selection. The library approach revealed stable heterodimeric sequences that were not expected on the basis of current design ideas embodied in the PV hypothesis. In addition, the selection addressed complex demands for in vivo function that cannot yet be addressed sufficiently by rational design. The differences between the dimers obtained from in vivo selection and rational design suggested that the DHFR complementation assay selects not only for stability and heterospecificity, but also for folding. The selected pairs, especially WinZip-A2B1, are stable and specific in vitro and in vivo. Thus, the combination of rational library design and in vivo selection is currently the most powerful strategy in cases where in vivo applications are envisioned.

Biological Implications

Coiled coils are widely distributed in nature and widely used in protein design. Consequently, the studies presented here have important implications for designing oligomerization domains and for understanding protein pairing specificity. The complexity of the selected WinZip sequences implies that a simple tabulation of potential g/e′ ion pairs is unlikely to define the interactions among the many coiled coils encoded in any specific genome. The optimal charge placement in stable heterospecific coiled coils is a complicated function that is only partially explained by the PV hypothesis.

The presence of two predicted repulsive g/e′ ion pairs in WinZip-A2B1 unexpectedly caused only a small reduction in dimer stability and pairing specificity compared to VelA1-VelB1, which lacked predicted repulsive g/e′ ion pairs (Table 1). These results indicate that sequence context influences significantly the thermodynamic contributions of the g and e interactions. The PV hypothesis, however, is a qualitative idea that does not account for context effects. Consequently, our results suggest that defining the differential contributions of ionic interactions in coiled coils requires analysis of interactions within native sequences.

The fastest *E. coli* growth was conferred by DHFR fusions to the genetically selected WinZip-A2B1 dimerization domain. This finding implies that the alternative, rational design strategy embodied in the PV hypothesis encompasses only a subset of important interhelix interactions. The PV idea does not address many other aspects—such as the overall electrostatic potential, rela-

tive concentrations of partners, protease sensitivity, expression, localization, pairing kinetics, and adventitious interactions with other cellular proteins—that may influence function in vivo. As a result, selection strategies are crucial to obtain coiled coils, including peptide probes targeted for naturally occurring sequences [34], that are useful for in vivo applications.

Experimental Procedures

Cloning and Selection

The construction and cloning of the libraries have been described previously [19]. Briefly, in the two coiled-coil libraries, the e and g positions were randomized to Gln, Glu, Arg, and Lys and the central a position to Asn and Val (Figure 1). The b, c, and f positions were based on the coiled-coil sequences of c-Jun (library A) and c-Fos (library B) (Figure 2). The hydrophobic core contained Leu at the d positions and Val at the a positions except for a3, which encoded a 1:1 mixture of Val and Asn. The DNA libraries were synthesized using trinucleotide codons [21] for the varied positions. The plasmid LibA-DHFR[1] expresses library A fused to the N-terminal fragment of mDHFR. The plasmid LibB-DHFR[2:I114A] expresses library B fused to the C-terminal part of the DHFR fragment with the destabilizing mutation Ile114Ala [52] in order to increase the selection stringency.

Chain shuffling [20] was carried out by transforming BL21 cells harboring one plasmid (either WinZipA1-DHFR[1] or WinZipB1-DHFR[2:I114A]) from the clone WinZip-A1B1 with the complementary library (LibB-DHFR[2:I114A] or LibA-DHFR[1], respectively). Transformants were plated on M9 minimal medium in the presence of 1 μg/ml trimethoprim and 1 mM IPTG (isopropyl-β-D-thiogalactopyranoside). This procedure is named single-step selection. To increase the selection stringency, the single-step selection was combined with growth competition. For this purpose, the colonies from the single-step selection were pooled and passaged in liquid medium under selective conditions (M9 minimal medium with 1 μg/ml trimethoprim, 1 mM IPTG) over 12 passages (serial transfers). Library pools obtained before the first and after every second passage, as well as DNA from single colonies obtained after passages 6, 8, 10, and 12, were analyzed by DNA sequencing.

The DNA encoding VelA1 was obtained by gene synthesis using the oligonucleotides VelA1_prA-fwd: 5′-CTGGCATGCAGTCGACTA CTGTGGCGCAACTGGAGGAAAAGGTGAAAACCCTTCGTGCTGAG AATTATGAACTTAAGTCT-3′ and VelA1_prA-rev: 5′-GACTAGTG CTAGCAAGCTGGGCAACCTGCTCCTCCAAGCGCTGCACCTCAGA CTTAAGTTCATAATTCT-3′. These oligonucleotides carried the appropriate restriction sites (SalI/NheI) for cloning into the plasmid LibA-DHFR[1]. The DNA encoding VelB1 was obtained by PCR from WinZip-B1 using the primers VelB1_prB-fwd: 5′-CTGGCATGCAGTC GACCTCCGTTGACGAACTGCAGGCTGAGGTTGACCAGCTGG AGGACGAGAATTACGCTC-3′ and DHFR_prB-rev: 5′-GGACTA GTGCTAGCTTCTGACAGCTTTTCCAC-3′ and cloned into LibB-DHFR[2:I114A]. The constructs were verified by DNA sequencing.

Quantification of Sequencing Profiles

Sequencing profiles were obtained by automated sequencing using an ABI PRISM 377 DNA sequencer with the DNA sequencing analysis software from the manufacturer. To monitor the selection kinetics of the chain-shuffling experiments, library pools were sequenced after every second passage. Assuming a Gaussian curve, the peak area for each base at every randomized position was calculated from the normalized electropherograms by measuring the height and the width at half height. Reproducibility was very high, as indicated by essentially identical profiles after repeated sequencing. The background was calculated in the same way from nonrandomized positions. Background values, which were very low, were subtracted from the calculated peak areas. From the base distribution at each randomized triplet, the percentage of the trinucleotide codons used in the randomization scheme (CAG, GAG, AAG, and CGT) was estimated and related to the respective amino acid. The fraction of A and G in position 1 defined the populations of Glu and Lys, respectively. The fraction of Arg residues was defined by the relative amounts of G and T in the second and third positions, respectively. The fraction of Gln residues was obtained as the remainder.

Because the number of cell generations can vary with each competition passage, the rate of selection was quantified separately for both chain-shuffling experiments. For both categories, the core a3 position converged fastest to the final sequence, which was nearly 100% after the single-step selection (P0). The rate of convergence at the e and g positions was ranked into three categories. For the chain-shuffling experiment that converged to WinZip-A2B1, the first category contained positions where the final sequence was >45% after the second passage (P2) and >70% in P4. In the second category, the final sequence was <70% in P4, and in the third category, the final sequence was ≤45% in P4. For the chain-shuffling experiment that converged to WinZip-A1B2, the first category contained positions where the final sequence was ≥45% in P2 and ≥75% in P4. In the second category, the final sequence was <45% in P2 and ≥75% in P4. In the third category, the final sequence was <75% in P4.

Peptide Synthesis and Purification

Peptides corresponding to the chain-shuffling winners WinZip-A2 (Ac-STTVAQLRERVKTLRAQNYELESEVQRLREQVAQLAS-NH_2) and WinZip-B2 (Ac-STSVDELKAEVDQLQDQNYALRTKVAQLRKEVEK LSE-NH_2) and to the rationally improved winners VelA1 (Ac-STTVAQ LEEKVKTLRAENYELKSEVQRLEEQVAQLAS-NH_2) and VelB1 (Ac-ST SVDELQAEVDQLEDENYALKTKVAQLRKKVEKLSE-NH_2) were synthesized and purified as described for the peptides WinZip-A1 and WinZip-B1 [19]. The peptides were acetylated at the N terminus and amidated at the C terminus to resemble more closely the DHFR fusions. In addition, to allow helix capping and increase solubility, 3 N-terminal residues and 2 C-terminal residues were included (underlined), rather than starting and ending with a hydrophobic amino acid. These amino acids are identical to those flanking the coiled-coil sequences in the fusion proteins. Each peptide was purified by reverse-phase HPLC, and the amino acid composition was confirmed by mass spectrometry. Peptide concentrations were determined by tyrosine absorbance in 6 M GdnHCl [53].

Circular Dichroism

CD studies were performed with an Aviv model 62DS spectrometer. Spectra were measured at 5°C using a total peptide concentration of 150 μM in a 1 mm cuvette. The standard buffer was 10 mM potassium phosphate (pH 7.0), 100 mM KF, as used previously for the characterization of WinZip-A1B1 [19]. Thermal denaturation curves were measured at 222 nm from 0°C to 97.5°C in steps of 2.5°C (2 min equilibration, 30 s data averaging). Thermal transitions were ≥95% reversible. Apparent T_m values were determined by least squares fitting of the denaturation curves [54] assuming a two-state model (folded dimer, unfolded monomer). ΔT_m was calculated as T_m(heterodimer) − [T_m(homodimer A) + T_m(homodimer B)]/2. Urea denaturation equilibria were determined at 20°C by automated titration of native peptide in a 10 mm cuvette with denatured peptide in 6 M urea measuring the CD signal at 222 nm (300 s equilibration, 30 s data averaging). The peptide concentrations were 30 μM for WinZip-A1, -A2, -A1B1, -A1B2, -A2B1, VelA1, and VelA1-VelB1. For the less stable homodimers, higher concentrations were chosen (40 μM for WinZip-B2 and 60 μM for WinZip-B1 and VelB1). K_D values were calculated by linear extrapolation to 0 M denaturant assuming a two-state model (K_D = [unfolded monomer]^2/[folded dimer]). $\Delta\Delta G_{spec}$ values were calculated as ΔG(heterodimer) − [ΔG(homodimer A) + ΔG(homodimer B)]/2.

Native Gel Electrophoresis

Gels (7.5% polyacrylamide [acrylamide:bis-acrylamide = 19:1]), polymerized in 375 mM β-alanine acetate buffer [pH 4.5]) were run with 500 mM β-alanine acetate buffer (pH 4.5). Samples (~10 μg peptides per lane) were diluted 2-fold with 600 mM β-alanine acetate (pH 4.5), 0.2% (w/v) methyl green, 30% glycerol. Gels were prerun at 100 V for at least 45 min and run for 2–3 hr at 5°C. Gels were fixed with 2% glutaraldehyde before staining with Coomassie blue.

Quantification of Cell Growth

For comparison of cell growth on agar plates, an overnight culture (M9 minimal medium with 1 μg/ml trimethoprim, 1 mM IPTG) was

inoculated from a glycerol stock prepared from a single colony grown under selective conditions. A second liquid culture was started from the overnight culture with a starting OD_{600} of 0.005 and grown for several hours until the OD_{600} was high enough to be measured accurately but low enough that the cells were still in logarithmic growth (between 0.05 and 0.7). An aliquot containing 300–600 cells was plated on freshly prepared agar plates (M9 minimal medium with 1 μg/ml trimethoprim, 1 mM IPTG). The plates were incubated for 56 hr at 37°C or 60 hr at 30°C or 42°C, respectively, to yield approximately the same range of colony sizes at each temperature. The plates were scanned at 600 dots per inch, and the colony area was quantified using the program NIH image. Overlapping colonies were deleted from the image before quantification. Growth in liquid culture was started from cultures in exponential growth. To achieve this condition, overnight cultures (M9 minimal medium with 1 μg/ml trimethoprim, 1 mM IPTG) were inoculated from the glycerol stock using different dilutions. An overnight culture with an OD_{600} of about 0.1 was used to inoculate a 50 ml culture in M9 minimal medium containing 1 μg/ml trimethoprim, 1 mM IPTG to a starting OD_{600} of 0.001. The OD_{600} was measured every hour during growth at 37°C, and the doubling time was calculated for the exponential phase. Each strain was measured in triplicate or quadruplicate, and the precision of the data was assessed by carrying out two independent experiments.

Acknowledgments

K.M.A. was a recipient of a PhD grant from the Roche Research Foundation (formerly Stipendienfonds der Basler Chemischen Industrie). J.N.P. was a recipient of a fellowship from le Conseil de Recherches en Science Naturelles et en Génie du Canada and is currently a research professor of les Fonds pour la Formation de Chercheurs et l'Aide à la Recherche. K.M.M. was a recipient of a postdoctoral fellowship from the Schweizerischer Nationalfonds and a long-term fellowship from the Human Frontier Science Program. This work was funded by NIH grant GM48958 (T.A.) and grant 0311628 from the German Bundesministerium für Bildung und Forschung (A.P.). We thank D. King for peptide synthesis and mass spectrometry, R. Schackmann for peptide synthesis, B. Klinger for help in some of the growth experiments, and Günter Wellnhofer (Morphosys AG, Munich, Germany) for the synthesis of the oligonucleotides with trinucleotides.

Received: April 25, 2002
Accepted: May 24, 2002

References

1. Müller, K.M., Arndt, K.M., and Plückthun, A. (1998). A dimeric bispecific miniantibody combines two specificities with avidity. FEBS Lett. *432*, 45–49.
2. Müller, K.M., Arndt, K.M., Strittmatter, W., and Plückthun, A. (1998). The first constant domain (C_H1 and C_L) of an antibody used as heterodimerization domain for bispecific miniantibodies. FEBS Lett. *422*, 259–264.
3. Cohen, C., and Parry, D.A. (1990). α-helical coiled coils and bundles: how to design an α-helical protein. Proteins *7*, 1–15.
4. Alber, T. (1992). Structure of the leucine zipper. Curr. Opin. Genet. Dev. *2*, 205–210.
5. Landschulz, W.H., Johnson, P.F., and McKnight, S.L. (1988). The leucine zipper: a hypothetical structure common to a new class of DNA binding proteins. Science *240*, 1759–1764.
6. O'Shea, E.K., Rutkowski, R., and Kim, P.S. (1989). Evidence that the leucine zipper is a coiled coil. Science *243*, 538–542.
7. Hodges, R.S. (1996). Boehringer Mannheim award lecture 1995. De novo design of α-helical proteins: basic research to medical applications. Biochem. Cell Biol. *74*, 133–154.
8. Hurst, H.C. (1995). Transcription factors 1: bZIP proteins. Protein Profile *2*, 101–168.
9. Müller, K.M., Arndt, K.M., and Alber, T. (2000). Protein fusions to coiled-coil domains. Methods Enzymol. *328*, 261–282.
10. Wolf, E., Kim, P.S., and Berger, B. (1997). MultiCoil: a program for predicting two- and three-stranded coiled coils. Protein Sci. *6*, 1179–1189.
11. Zeng, X., Herndon, A.M., and Hu, J.C. (1997). Buried asparagines determine the dimerization specificities of leucine zipper mutants. Proc. Natl. Acad. Sci. USA *94*, 3673–3678.
12. Harbury, P.B., Zhang, T., Kim, P.S., and Alber, T. (1993). A switch between two-, three-, and four-stranded coiled coils in GCN4 leucine zipper mutants. Science *262*, 1401–1407.
13. Hicks, M.R., Holberton, D.V., Kowalczyk, C., and Woolfson, D.N. (1997). Coiled-coil assembly by peptides with non-heptad sequence motifs. Fold. Des. *2*, 149–158.
14. O'Shea, E.K., Lumb, K.J., and Kim, P.S. (1993). Peptide 'Velcro': design of a heterodimeric coiled coil. Curr. Biol. *3*, 658–667.
15. Wendt, H., Leder, L., Harma, H., Jelesarov, I., Baici, A., and Bosshard, H.R. (1997). Very rapid, ionic strength-dependent association and folding of a heterodimeric leucine zipper. Biochemistry *36*, 204–213.
16. Graddis, T.J., Myszka, D.G., and Chaiken, I.M. (1993). Controlled formation of model homo- and heterodimer coiled coil polypeptides. Biochemistry *32*, 12664–12671.
17. Zeng, X., Zhu, H., Lashuel, H.A., and Hu, J.C. (1997). Oligomerization properties of GCN4 leucine zipper e and g position mutants. Protein Sci. *6*, 2218–2226.
18. Pu, W.T., and Struhl, K. (1993). Dimerization of leucine zippers analyzed by random selection. Nucleic Acids Res. *21*, 4348–4355.
19. Arndt, K.M., Pelletier, J.N., Müller, K.M., Alber, T., Michnick, S.W., and Plückthun, A. (2000). A heterodimeric coiled-coil peptide pair selected in vivo from a designed library-versus-library ensemble. J. Mol. Biol. *295*, 627–639.
20. Pelletier, J.N., Arndt, K.M., Plückthun, A., and Michnick, S.W. (1999). An in vivo library-versus-library selection of optimized protein-protein interactions. Nat. Biotechnol. *17*, 683–690.
21. Virnekäs, B., Ge, L., Plückthun, A., Schneider, K.C., Wellnhofer, G., and Moroney, S.E. (1994). Trinucleotide phosphoramidites: ideal reagents for the synthesis of mixed oligonucleotides for random mutagenesis. Nucleic Acids Res. *22*, 5600–5607.
22. O'Neil, K.T., and DeGrado, W.F. (1990). A thermodynamic scale for the helix-forming tendencies of the commonly occurring amino acids. Science *250*, 646–651.
23. Chen, Y.H., Yang, J.T., and Chau, K.H. (1974). Determination of the helix and β form of proteins in aqueous solution by circular dichroism. Biochemistry *13*, 3350–3359.
24. Hendsch, Z.S., Nohaile, M.J., Sauer, R.T., and Tidor, B. (2001). Preferential heterodimer formation via undercompensated electrostatic interactions. J. Am. Chem. Soc. *123*, 1264–1265.
25. Hendsch, Z.S., and Tidor, B. (1999). Electrostatic interactions in the GCN4 leucine zipper: substantial contributions arise from intramolecular interactions enhanced on binding. Protein Sci. *8*, 1381–1392.
26. McCoy, A.J., Chandana Epa, V., and Colman, P.M. (1997). Electrostatic complementarity at protein/protein interfaces. J. Mol. Biol. *268*, 570–584.
27. Nohaile, M.J., Hendsch, Z.S., Tidor, B., and Sauer, R.T. (2001). Altering dimerization specificity by changes in surface electrostatics. Proc. Natl. Acad. Sci. USA *98*, 3109–3114.
28. John, M., Briand, J.P., Granger-Schnarr, M., and Schnarr, M. (1994). Two pairs of oppositely charged amino acids from Jun and Fos confer heterodimerization to GCN4 leucine zipper. J. Biol. Chem. *269*, 16247–16253.
29. Nautiyal, S., Woolfson, D.N., King, D.S., and Alber, T. (1995). A designed heterotrimeric coiled coil. Biochemistry *34*, 11645–11651.
30. Nautiyal, S., and Alber, T. (1999). Crystal structure of a designed, thermostable, heterotrimeric coiled coil. Protein Sci. *8*, 84–90.
31. O'Shea, E.K., Rutkowski, R., and Kim, P.S. (1992). Mechanism of specificity in the Fos-Jun oncoprotein heterodimer. Cell *68*, 699–708.
32. Beck, K., Dixon, T.W., Engel, J., and Parry, D.A. (1993). Ionic interactions in the coiled-coil domain of laminin determine the specificity of chain assembly. J. Mol. Biol. *231*, 311–323.
33. Nomizu, M., Utani, A., Beck, K., Otaka, A., Roller, P.P., and Yamada, Y. (1996). Mechanism of laminin chain assembly into

a triple-stranded coiled-coil structure. Biochemistry *35*, 2885–2893.

34. Sharma, V.A., Logan, J., King, D.S., White, R., and Alber, T. (1998). Sequence-based design of a peptide probe for the APC tumor suppressor protein. Curr. Biol. *8*, 823–830.
35. O'Shea, E.K., Klemm, J.D., Kim, P.S., and Alber, T. (1991). X-ray structure of the GCN4 leucine zipper, a two-stranded, parallel coiled coil. Science *254*, 539–544.
36. Day, C.L., and Alber, T. (2000). Crystal structure of the amino-terminal coiled-coil domain of the APC tumor suppressor. J. Mol. Biol. *301*, 147–156.
37. Kammerer, R.A., Jaravine, V.A., Frank, S., Schulthess, T., Landwehr, R., Lustig, A., Garcia-Echeverria, C., Alexandrescu, A.T., Engel, J., and Steinmetz, M.O. (2001). An intrahelical salt bridge within the trigger site stabilizes the GCN4 leucine zipper. J. Biol. Chem. *276*, 13685–13688.
38. Hwang, J.K., and Warshel, A. (1988). Why ion pair reversal by protein engineering is unlikely to succeed. Nature *334*, 270–272.
39. Kohn, W.D., Kay, C.M., and Hodges, R.S. (1998). Orientation, positional, additivity, and oligomerization-state effects of interhelical ion pairs in α-helical coiled-coils. J. Mol. Biol. *283*, 993–1012.
40. Krylov, D., Mikhailenko, I., and Vinson, C. (1994). A thermodynamic scale for leucine zipper stability and dimerization specificity: e and g interhelical interactions. EMBO J. *13*, 2849–2861.
41. Muñoz, V., and Serrano, L. (1997). Development of the multiple sequence approximation within the AGADIR model of α-helix formation: comparison with Zimm-Bragg and Lifson-Roig formalisms. Biopolymers *41*, 495–509.
42. Lacroix, E., Viguera, A.R., and Serrano, L. (1998). Elucidating the folding problem of α-helices: local motifs, long-range electrostatics, ionic-strength dependence and prediction of NMR parameters. J. Mol. Biol. *284*, 173–191.
43. Yu, Y., Monera, O.D., Hodges, R.S., and Privalov, P.L. (1996). Investigation of electrostatic interactions in two-stranded coiled-coils through residue shuffling. Biophys. Chem. *59*, 299–314.
44. Spek, E.J., Bui, A.H., Lu, M., and Kallenbach, N.R. (1998). Surface salt bridges stabilize the GCN4 leucine zipper. Protein Sci. *7*, 2431–2437.
45. Zitzewitz, J.A., Ibarra-Molero, B., Fishel, D.R., Terry, K.L., and Matthews, C.R. (2000). Preformed secondary structure drives the association reaction of GCN4-p1, a model coiled-coil system. J. Mol. Biol. *296*, 1105–1116.
46. Moran, L.B., Schneider, J.P., Kentsis, A., Reddy, G.A., and Sosnick, T.R. (1999). Transition state heterogeneity in GCN4 coiled coil folding studied by using multisite mutations and crosslinking. Proc. Natl. Acad. Sci. USA *96*, 10699–10704.
47. Dahiyat, B.I., Gordon, D.B., and Mayo, S.L. (1997). Automated design of the surface positions of protein helices. Protein Sci. *6*, 1333–1337.
48. Kohn, W.D., Kay, C.M., and Hodges, R.S. (1997). Positional dependence of the effects of negatively charged Glu side chains on the stability of two-stranded α-helical coiled-coils. J. Pept. Sci. *3*, 209–223.
49. Kohn, W.D., Kay, C.M., and Hodges, R.S. (1995). Protein destabilization by electrostatic repulsions in the two-stranded α-helical coiled-coil/leucine zipper. Protein Sci. *4*, 237–250.
50. Jelesarov, I., and Bosshard, H.R. (1996). Thermodynamic characterization of the coupled folding and association of heterodimeric coiled coils (leucine zippers). J. Mol. Biol. *263*, 344–358.
51. Arndt, K.M., Müller, K.M., and Plückthun, A. (2001). Helix-stabilized Fv (hsFv) antibody fragments: substituting the constant domains of a Fab fragment for a heterodimeric coiled-coil domain. J. Mol. Biol. *312*, 221–228.
52. Pelletier, J.N., Campbell-Valois, F.X., and Michnick, S.W. (1998). Oligomerization domain-directed reassembly of active dihydrofolate reductase from rationally designed fragments. Proc. Natl. Acad. Sci. USA *95*, 12141–12146.
53. Edelhoch, H. (1967). Spectroscopic determination of tryptophan and tyrosine in proteins. Biochemistry *6*, 1948–1954.
54. Becktel, W.J., and Schellman, J.A. (1987). Protein stability curves. Biopolymers *26*, 1859–1877.